

Anomalous ^{125}Te Nuclear Spin Relaxation Coincident with Charge Kondo Behavior in Superconducting $\text{Pb}_{1-x}\text{Tl}_x\text{Te}$

Hidekazu Mukuda^{1*}, Takashi Matsumura¹, Shota Maki¹, Mitsuharu Yashima¹, Yoshio Kitaoka¹, Kazumasa Miyake², Hironaru Murakami³, Paula Giraldo-Gallo⁴, Theodore H. Geballe⁴, and Ian R. Fisher⁴

¹Graduate School of Engineering Science, Osaka University, Toyonaka, Osaka 560-8531, Japan

²Center for Advanced High Magnetic Field Science, Osaka University, Osaka 560-0043, Japan

³Institute of Laser Engineering, Osaka University, Suita, Osaka 565-0871, Japan

⁴Department of Applied Physics, Stanford University, California 94305, USA

(Received June 21, 2021)

We report the results of a ^{125}Te NMR study of single crystalline $\text{Pb}_{1-x}\text{Tl}_x\text{Te}$ ($x=0, 0.35, 1.0\%$) as a window on the novel electronic states associated with the thallium impurities in PbTe . The Knight shift is enhanced as x increases, corresponding to an increase in the average density of states (DOS) coupled to a strong spatial variation in the local DOS surrounding each Tl dopant. Remarkably, for the superconducting composition ($x=1.0\%$), the ^{125}Te nuclear spin relaxation rate ($1/T_1T$) for Te ions that are close to the Tl dopants is unexpectedly enhanced in the normal state below a characteristic temperature of ~ 10 K, below which the resistivity experiences an upturn. Such a simultaneous upturn in both the resistivity and ($1/T_1T$) was not suppressed in the high magnetic field. We suggest that these observations are consistently accounted for by dynamical charge fluctuations in the absence of paramagnetism, which is anticipated by the charge Kondo scenario associated with the Tl dopants. In contrast, such anomalies were not detected in the non-superconducting samples ($x=0$ and 0.35%), suggesting a connection between dynamical valence fluctuations and the occurrence of superconductivity in $\text{Pb}_{1-x}\text{Tl}_x\text{Te}$.

Low-carrier-density superconductors provide a challenge to the conventional Bardeen-Cooper-Schrieffer (BCS) theory of superconductivity. Moreover, such materials potentially provide clues for ways to boost the critical temperature of other, more conventional, materials. Here, we investigate via NMR measurements the local electronic properties of one such anomalous low-carrier-density superconductor, $\text{Pb}_{1-x}\text{Tl}_x\text{Te}$. PbTe is a narrow-gap semiconductor. Small amounts of substitution of Tl for Pb (i.e., $\text{Pb}_{1-x}\text{Tl}_x\text{Te}$) lead to a superconducting (SC) ground state when x exceeds $x_c \sim 0.3\%$.¹⁻⁴ Significantly, thallium is the only dopant known to cause superconductivity in PbTe , suggesting that these specific impurities have a unique effect on the electronic states near the Fermi energy. Although the carrier densities are $\lesssim 10^{20}\text{cm}^{-3}$, the SC transition temperature rises to $T_c \sim 1.5$ K for $x \sim 1.5\%$ (the solubility limit), higher than that of other well-known low-carrier-density superconductors, such as SrTiO_3 .⁵ The hole density p , estimated by Hall coefficient measurements, increases linearly with x for compositions up to $x \sim x_c$, implying that each Tl impurity acts as an acceptor, having a formal valence Tl^{1+} . However, as x increases further, the increase in p gradually saturates, implying that impurities no longer contribute one hole per dopant. Drawing on the known valence-skipping character of thallium ions,⁶ this behavior has been interpreted in terms of the onset of a degeneracy of impurity states with a formal valence of Tl^{1+} (hole doping) and Tl^{3+} (electron doping) for $x > x_c$.^{2-4,7} Indirect support for such a scenario was obtained via the observation of a logarithmic upturn in

the resistivity at low temperatures for $x > x_c$, reminiscent of the Kondo effect,⁸ but in the absence of unpaired spins.^{4,9} This observation was interpreted as evidence for a *charge* Kondo effect, that is, a Kondo effect arising from the interaction of the conduction electrons with the two degenerate valence states of the Tl dopants.^{4,10-14} The fact that such an effect is observed only for SC compositions^{4,15} implies that valence fluctuations might play a key role in the pairing interaction in $\text{Pb}_{1-x}\text{Tl}_x\text{Te}$, possibly explaining the high critical temperatures found in this system.^{6,10-14} Motivated by these bulk experiments and theoretical insights, we investigated the *local* electronic states around Tl dopants by means of ^{125}Te -NMR from the microscopic point of view.

In this Letter, we report a systematic ^{125}Te -NMR study on $\text{Pb}_{1-x}\text{Tl}_x\text{Te}$, revealing the unusual character of the local electronic states introduced by Tl dopants through systematic measurements of the Knight shift (K) and the nuclear spin relaxation rate ($1/T_1T$). Our main result is that ($1/T_1T$) is found to be significantly enhanced below 10 K at Te sites in the vicinity of the Tl dopants for the SC sample ($x=1.0\%$), whereas no such anomalous enhancement is seen for $x = 0$ (the non-SC parent compound) or $x \sim 0.35\%$ (i.e., $x \sim x_c$). The temperature at which ($1/T_1T$) is enhanced for the SC composition coincides with the temperature below which the normal state resistivity experiences an upturn. We suggest that such a simultaneous upturn in both the resistivity and ($1/T_1T$) can be consistently understood in terms of the coherent charge fluctuations anticipated in the charge Kondo effect.

High-quality single crystals of $\text{Pb}_{1-x}\text{Tl}_x\text{Te}$ with $x=0$,

*E-mail: mukuda@mp.es.osaka-u.ac.jp

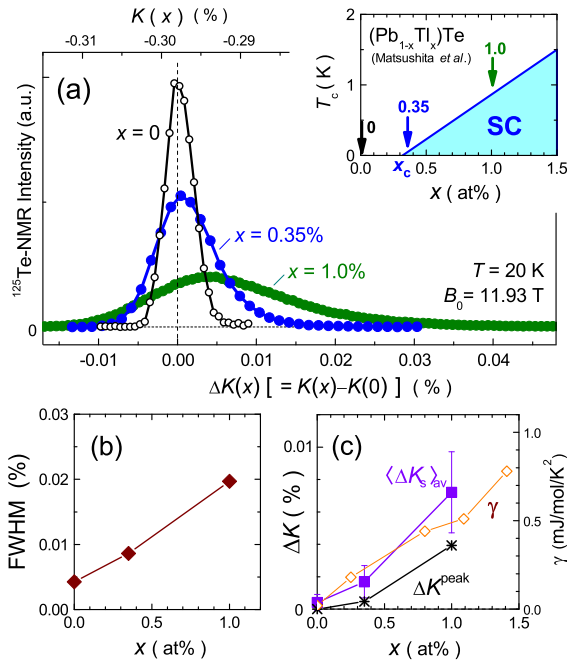


Fig. 1. (Color online) (a) ^{125}Te -NMR spectra at $T=20$ K for $x=0$, 0.35, and 1.0%. Here, the horizontal axis $\Delta K(x)$ is defined as $K(x) - K(0)$, which represents the relative shift from that of $x=0$. The arrows in the inset indicate the samples measured in this work, plotted on the SC phase diagram reported previously.⁴ (b) The FWHM of the spectra, expressed as a scale of $K(x)$, and (c) ΔK^{peak} and $\langle \Delta K_s \rangle_{\text{av}}$ defined by the peak and the center of gravity of the spectra, respectively, as a function of thallium concentration, x . The x dependence of the Sommerfeld coefficient (γ) in specific heat is cited from Ref.⁷

0.35, and 1.0% were grown by an unseeded physical vapor transport method, as described previously.⁴ Thallium concentrations were determined for other crystals from the same growth batches by an electron microprobe analysis with an estimated uncertainty of $\sim \pm 0.1\%$.⁴ The crystals of $x=0.35$ and 1.0% correspond to the borderline region of the SC phase ($x \simeq x_c$) and the SC region ($x > x_c$) with $T_c \sim 1$ K, respectively, as shown by the arrows in the inset of Fig. 1(a).⁴ Resistivity measurements for these samples reproduce previous results,⁴ including the upturn below ~ 10 K for $x=1\%$ (see inset of Fig. 3). ^{125}Te -NMR ($I=1/2$) measurements of the Knight shift ($K = (f - \gamma_n B_0)/\gamma_n B_0$) and the nuclear spin-lattice relaxation rate ($1/T_1$) were performed on coarsely ground crystals of all three compositions in a magnetic field of $B_0 \sim 11.93$ T. Here, γ_n is the nuclear gyromagnetic ratio, and f is the frequency. T_1 was obtained by fitting a recovery curve for ^{125}Te nuclear magnetization to a single exponential function, $m(t) \equiv [M_0 - M(t)]/M_0 = \exp(-t/T_1)$, where M_0 and $M(t)$ are the nuclear magnetizations for a thermal equilibrium condition and at time t after a saturation pulse, respectively.

First, we focus on the doping effect on the static electronic properties through the measurement of K . Figure 1(a) shows the ^{125}Te -NMR spectra at $T=20$ K for $x=0$, 0.35, and 1.0%. Here, the frequency on the horizontal axis is converted to the scale of the Knight shift $K(x)$, and

$\Delta K(x) = K(x) - K(0)$ represents the relative shift from that of undoped $x=0$ (bottom axis). The full-width at half-maximum (FWHM) of the spectra becomes large with increasing x , as shown in Fig. 1(b). The spectra are nevertheless composed of a single peak even for the doped samples, indicating that the doped Tl atoms are distributed randomly throughout the samples, excluding the possibility of dopant clusters and/or decomposition. The doping of the Tl atoms causes $\Delta K(x)$ to increase, as shown in Fig. 1(c) by ΔK^{peak} determined by the peak of spectra. In general, the observed $K(x)$ comprises the spin shift K_s and the chemical shift K_{chem} . The former K_s is proportional to $A_{\text{hf}}\chi_0 \propto A_{\text{hf}}N_0$, where χ_0 is the static spin susceptibility at $q=0$, A_{hf} is the hyperfine coupling constant, and N_0 is the density of states (DOS) at the Fermi level (E_F). Since K_{chem} is independent of x in a small range, $\Delta K(x) [\equiv K(x) - K(0)]$ corresponds to their spin components $\Delta K_s(x) [\equiv K_s(x) - K_s(0)]$. Hence, in Fig. 1(c), the increase in ΔK^{peak} with Tl doping originates from that of χ_0 or N_0 at the Te sites in the vicinity of the Tl dopants. It is noteworthy that, as indicated in Fig. 1(a), the FWHM in the spectrum is significantly increased toward the *positive* side in $\Delta K(x)$ with increasing x . The fraction of Te ions (relative to the total number of Te ions) that are nearest neighbors to a Tl dopant increases as x increases; accordingly, the Te sites closer to the Tl dopants possess the larger $\Delta K_s(x)$ or the larger N_0 relative to those that are farther from the Tl dopants. In this context, the spatially averaged value of ΔK_s at the Te sites should be evaluated by $\langle \Delta K_s \rangle_{\text{av}}$, which is defined by the center of gravity of the broad spectrum, as shown in Fig. 1(c). The x dependence of $\langle \Delta K_s \rangle_{\text{av}}$ is comparable to that of the N_0 value estimated by the Sommerfeld coefficient (γ) in specific heat measurements.⁷ The close correspondence between these two spatially averaged values confirms our interpretation of the physical origin of $\Delta K(x)$. It also indicates that K_{chem} is assumed to be constant for the present x region. We emphasize that the large distribution of $\Delta K_s(x)$ with increasing x is indicative of a strong spatial variation in the local DOS surrounding each Tl dopant, which is especially pronounced for the larger Tl concentrations.

Next, we address the evolution of the local electronic states introduced by the Tl dopants through the ^{125}Te nuclear spin lattice relaxation rate, $1/T_1$. Figure 2(a) shows $(1/T_1 T)$ for $x=1.0\%$ at $T=3.6$ and 20 K, which are measured at the Te sites denoted by A_i ($i=1$ to 6) in the spectrum (defined in the upper panel of the same figure). Each T_1 value for each A_i is determined from the dominant component in the recovery curve $m(t)$, shown by solid lines in Fig. 2(c). Note that the values of ΔK are widely distributed over the sample, which allows us to examine the local electronic characteristics at the different distances from the Tl dopants. In particular, we find that values of $(1/T_1 T)$ become progressively larger for larger values of ΔK . This is in sharp contrast to the undoped ($x=0$) case, which exhibits a homogeneous value of $1/T_1$ for all Te sites. It should be noted that the large values of $(1/T_1 T)$ at the large values of ΔK originate from the Te sites in the vicinity of the Tl dopants, which is indicative of a significant change in the local electronic state

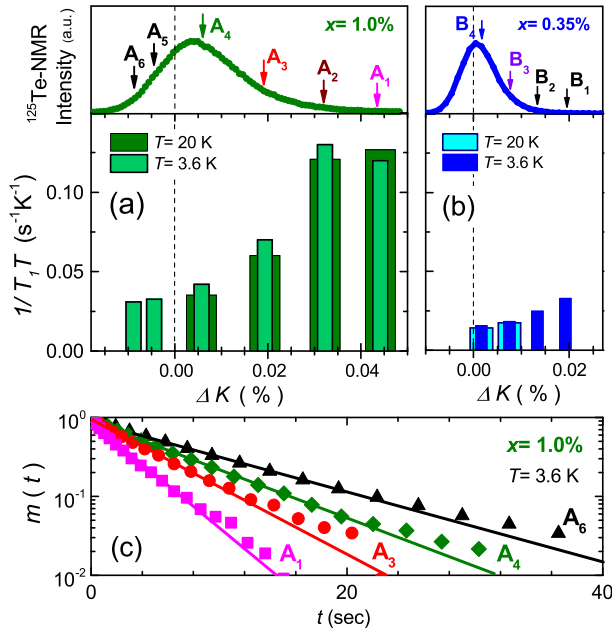


Fig. 2. (Color online) $(1/T_1T)$ for (a) $x=1.0\%$ and (b) $x=0.35\%$ measured as a function of ΔK , corresponding to A_i ($i=1$ to 6) and B_i ($i=1$ to 4) denoted in the upper panels, respectively. (c) Recovery curves of nuclear magnetization $m(t)$ for A_i ($i=1$ to 6), the slope of which enables us to evaluate T_1 . Representative data are shown here for the sample with $x=1.0\%$ at $T \sim 3.6$ K. The large $(1/T_1T)$ value that is shown here for the larger values of ΔK is not observed in samples with $x=0$ and is therefore due to the presence of Tl dopants.

induced by doping Tl atoms. In contrast, for $x=0.35\%$ the distributions at the Te sites denoted by B_i ($i=1$ to 4) are also significant but smaller than those for $x=1.0\%$, as shown in Fig. 2(b). This shows that the presence of Tl dopants increases the distributions in $(1/T_1T)$ and ΔK with increasing $x(>0)$.

In order to gain further insight into the unique electronic state induced by Tl dopants, and the difference between SC and non-SC compositions, the temperature (T) dependence of $(1/T_1T)$ was measured as shown in Fig. 3. For $x=0.35\%$ ($x \simeq x_c$), $(1/T_1T)=const.$ is observed at B_4 and B_3 in the T range of 1.4–60 K, as anticipated for a typical metal. In sharp contrast, for $x=1.0\%$ ($x > x_c$), the $(1/T_1T)$ values at A_1 , A_2 , and A_3 (i.e., in the vicinity of the Tl dopants) start to increase dramatically below $T_{\min}^{\text{NMR}} \simeq 10$ K. Significantly, $T_{\min}^{\text{NMR}} \simeq 10$ K coincides with T_{\min}^{ρ} , the temperature below which the resistivity experiences a logarithmic upturn,⁴ as shown in the inset of Fig. 3. By contrast, such an increase in $(1/T_1T)$ at A_i ($i=1-3$) is largely suppressed at A_4 , which corresponds to Te sites that are located far from the Tl dopants. These results reveal that the anomalous enhancement in $(1/T_1T)$ is only seen for Te sites close to Tl dopants for $x=1.0\%$ in the SC compositions. It is especially unusual that the upturn in $(1/T_1T)$ is observed for the more heavily doped composition ($x=1.0\%$), whereas typically for doped semiconductors one anticipates that $(1/T_1T) = const.$ for more heavily doped compositions close to the normal metallic state.¹⁶ We note that in some cases of slightly doped

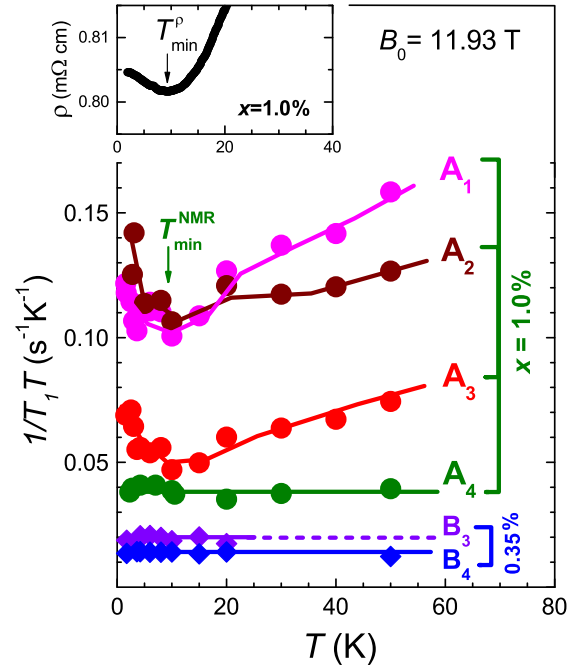


Fig. 3. (Color online) T dependence of $(1/T_1T)$ for $x=1.0$ and 0.35% measured at ΔK denoted as A_i and B_i , respectively (see the upper panels of Figs. 2(a) and 2(b) for definitions of A_i and B_i). The anomalous increases in $(1/T_1T)$ below $T_{\min}^{\text{NMR}} \sim 10$ K for $x=1.0\%$ are only seen for A_i ($i=1,2,3$), corresponding to the Te sites close to the Tl dopants. Inset shows the Kondo-like resistivity upturn below $T_{\min}^{\rho} \sim 10$ K observed in the present ($x = 1.0\%$) sample.⁴

semiconductors^{17–19} a Curie-Weiss-like temperature dependence of $(1/T_1T)$ was observed at low fields due to the magnetization of the impurity states, but they are suppressed by high fields. Thus, the simultaneous low-temperature upturn in both the resistivity and $(1/T_1T)$ even for heavily doped compositions and the lack of suppression of the upturn by the application of a field of 12 T are the unique features in $\text{Pb}_{1-x}\text{Tl}_x\text{Te}$. This differs from the case of the simple dilute “spin” Kondo effect with a low Kondo temperature. Furthermore, the increase in $(1/T_1T)$ should be attributed to the local anomaly from the presence of Tl dopants because it is seen only at Te sites close to Tl dopants, and hence it also differs from the usual $q \neq 0$ magnetic excitation pictures. These features put $\text{Pb}_{1-x}\text{Tl}_x\text{Te}$ in a distinct new class of doped semiconductors.

The observation of a logarithmic upturn in the resistivity below 10 K for $x > x_c$ is reminiscent of the Kondo effect,⁸ but apparently in the absence of magnetic impurities.^{4,9} It was previously suggested that this behavior could be accounted for by a “charge” Kondo effect,^{6,10–14} in which fluctuations between the two degenerate charge states of the Tl impurities (i.e. $2e^-(\text{Tl}^{1+})$ and $0e^-(\text{Tl}^{3+})$ for $x > x_c$) are screened by the free carriers, analogous with the screening of fluctuations between two degenerate spin states in the conventional “spin” Kondo effect. Our experimental results further support this hypothesis. First, our data provide microscopic evidence that (a) the static spin susceptibility χ_0 deduced from ΔK shows

no apparent T dependence in the T range $1.8 \text{ K} < T < 50 \text{ K}$, and (b) that the upturn in $(1/T_1T)$ upon cooling below 10 K is not suppressed even by the application of a strong magnetic field of $\sim 12 \text{ T}$, both of which are consistent with the absence of spin degrees of freedom. Second, Miyake *et al.* have pointed out recently that the observed enhancement in $(1/T_1T)$ below T_{\min}^{NMR} can be readily understood within the charge Kondo picture as the result of the T dependence of the electron-pair hopping (EPH) interaction J_{ph} between $6s$ pair electrons on the Tl dopants and the conduction electrons.^{13, 20} That is, there exists a process contributing to $(1/T_1T)$ at the Te site, which is proportional to the EPH interaction J_{ph} . This EPH interaction is transformed to the spin exchange interaction J_{\perp} by a particle-hole transformation for the down spin component of both the $6s$ and conduction electrons. The renormalized $J_{\perp}(T)$ (or J_{ph}) by the Kondo effect exhibits a logarithmic T dependence at $T \gtrsim T_{\text{K}}$ (Kondo temperature),²¹ like $J_{\perp}(T) = J_{\perp}^{\infty}/[1 + J_{\perp}^{\infty}N_0 \log(T/D)] \approx -(J_{\perp}^{\infty})^2N_0 \log(T/D)$, where J_{\perp}^{∞} and D are the bare exchange interaction and the half-bandwidth of the conduction band, respectively. In addition, this scenario also reproduces no apparent T dependence of the static susceptibility observed by the Knight shift. These observations are consistently accounted for by the dynamical charge fluctuations in the absence of paramagnetism, which are anticipated by a charge Kondo scenario associated with the Tl dopants. In contrast, such anomalies in $(1/T_1T)$ were not detected for the non-SC parent ($x=0$) and for the composition close to x_c ($x \sim 0.35\%$). Our observations therefore provide a microscopic insight into the previously suggested connection between dynamical valence fluctuations and the occurrence of superconductivity in this material system.^{10–14}

Thus far we have focused on the strong spatial dependence of the Knight shift and $(1/T_1T)$ as a function of the distance to a Tl impurity, and on the T dependence of these quantities for temperatures below $T_{\min}^{\text{NMR}} \sim 10 \text{ K}$. An additional anomalous aspect of the data shown in Fig. 3 for the SC composition is the high- T behavior in $1/T_1T$ above T_{\min}^{NMR} . That is, we find that $1/T_1T$ increases up to $T \sim 50 \text{ K}$, but only for the Te sites at A_i ($i=1,2,3$) in the vicinity of the Tl dopants, while remaining constant as a function of temperature for the Te sites (A_4) far from the Tl dopants. The precise microscopic origin of this effect is not yet known. However, since this is a local anomaly enhanced around the Tl dopants, it should certainly be attributed to these impurities. An intriguing possibility is that this effect is related to the crossover from a coherent resonating valence state below T_{\min}^{NMR} to incoherent excited valence states at high T .¹³ Such a crossover would strongly affect the temperature dependence of the relaxation process. Further measurements directly probing the spin dynamics on the Tl sites might provide further insight into this behavior.

Finally, we comment on the relation of our observations to recent band structure calculations that aim to elucidate the nature of Tl impurities in PbTe. These calculations have revealed deep and resonant states formed from the hybridization of Tl impurities with coordinat-

ing Te ions.^{22, 23} Such states preserve much of the character of the original Tl wavefunctions, exhibiting similar behavior as virtual bound states. For small Tl concentrations ($x < x_c$), the Fermi energy is higher in the valence band than the resonant impurity levels.²³ Hole doping moves the Fermi energy deeper into the valence band, and earlier heat capacity data for double-doped systems indicate that the Fermi energy eventually resides in the resonant impurity levels for superconducting compositions.^{3, 15} Significantly, our measurements provide direct microscopic evidence for the anticipated spatial variation in DOS associated with such resonant impurity states. Moreover, we have shown that the nuclear spin dynamics are very different when the Fermi energy lies in the resonant impurity levels (i.e. for $x \sim 1.0\%$) relative to when it lies farther away from them ($x \sim 0.35\%$). The charge Kondo behavior suggested in the resistivity, and here in our NMR data, imply that the resonant impurity states at the Fermi energy are characterized by a negative effective U , consistent with the strongly Tl character of the associated orbitals^{22, 23} and expectations for this valence-skipping element.⁶

In summary, systematic measurements of the ^{125}Te NMR Knight shift and $(1/T_1T)$ on $\text{Pb}_{1-x}\text{Tl}_x\text{Te}$ have revealed that the Tl dopants induce spatially inhomogeneous electronic states around the Tl dopants. In the SC sample with $x=1.0\%$, a remarkable increase in $(1/T_1T)$ is observed upon cooling below 10 K for the Te sites close to the Tl dopants. The upturn in the resistivity is corroborated by a microscopic probe of $(1/T_1T)$. A simultaneous upturn in these values is not suppressed by the application of a high field. Such unique features can be understood consistently in terms of coherent charge fluctuations anticipated in the charge Kondo effect arising from the Tl impurities. In contrast, such an anomaly was not detected in non-SC samples with $x=0$ and 0.35% ($x \sim x_c$). Although the link between resonant impurity levels, valence fluctuations, and charge Kondo behavior has been discussed previously for this material,^{6, 10–14} these specific measurements are important in terms of providing the first microscopic insight into such a scenario. Although it has been established from a theoretical perspective that valence fluctuations can provide an effective pairing interaction,^{6, 10–14} it remains to be seen to what extent this is helpful for understanding the high critical temperature in this remarkable superconductor.

We thank H. Matsuura for his valuable comments. This work was supported by Izumi Science and Technology Foundation, Toyota Riken Scholar, and JSPS KAKENHI (Grant Nos. 26400356, 26610102, 16H04013, 25400369, and 17K05555). The work at Stanford University was supported by AFOSR Grant No. FA9550-09-1-0583.

- 1) I. A. Chernik, and S. N. Lykov, *Sov. Phys. Solid State* **23**, 817 (1981).
- 2) H. Murakami, W. Hattori, and R. Aoki, *Physica C(Amsterdam)* **269**, 83 (1996).
- 3) S. A. Némov and Y. I. Ravich, *Phys. Usp.* **41**, 735 (1998).
- 4) Y. Matsushita, H. Bluhm, T. H. Geballe, and I. R. Fisher, *Phys. Rev. Lett.* **94**, 157002 (2005).
- 5) J. F. Schooley, W. R. Hosler, and M. L. Cohen, *Phys. Rev.*

- Lett. **12**, 474 (1964).
- 6) C. M. Varma, Phys. Rev. Lett. **61**, 2713 (1988).
 - 7) Y. Matsushita, P. A. Wiannecki, A. T. Sommer, T. H. Geballe, and I. R. Fisher, Phys. Rev. B **74**, 134512 (2006).
 - 8) J. Kondo, Prog. Theor. Phys. **32**, 37 (1964).
 - 9) K. I. Andronik, V. F. Banar, V. G. Kantser, and A. S. Sidorenko, Phys. Status Solidi B **133**, K61 (1986).
 - 10) A. Taraphder and P. Coleman, Phys. Rev. Lett. **66**, 2814 (1991).
 - 11) M. Dzero and J. Schmalian, Phys. Rev. Lett. **94**, 157003 (2005).
 - 12) T. A. Costi and V. Zlatic, Phys. Rev. Lett. **108**, 036402 (2012).
 - 13) H. Matsuura and K. Miyake, J. Phys. Soc. Jpn. **81**, 113705 (2012).
 - 14) T. Yanagisawa and I. Hase, Physica C **494**, 24 (2013).
 - 15) A. S. Erickson, N. P. Breznay, E. A. Nowadnick, T. H. Geballe, and I. R. Fisher, Phys. Rev. B. **81**, 134521 (2010).
 - 16) E. M. Meintjes, J. Danielson, and W. W. Warren, Jr. , Phys. Rev. B. **71**, 035114 (2005).
 - 17) S. Kobayashi, Y. Fukagawa, S. Ikehata, and W. Sasaki, J. Phys. Soc. Jpn. **45**, 1276 (1978).
 - 18) S. Ikehata, T. Ema, K. Shun-ichi, and W. Sasaki, J. Phys. Soc. Jpn. **50**, 3655 (1981).
 - 19) S. Maeda, S. Katsube, and G.-q. Zheng, J. Phys. Soc. Jpn. **86**, 024702 (2017).
 - 20) K. Miyake and H. Matsuura, in preparation.
 - 21) P. W. Anderson, J. Phys. C **3**, 2436 (1970).
 - 22) S. Ahmad, S. D. Mahanti, K. Hoang, and M. G. Kanatzidis, Phys. Rev. B. **74**, 155205 (2006).
 - 23) K. Xiong, G. Lee, R. P. Gupta, W. Wang, B. E. Gnade and K. Cho, J. Phys. D: Appl. Phys. **43**, 405403 (2010).